ORIGINAL RESEARCH

Sugarcane bagasse and straw as low-cost lignocellulosic sorbents for the removal of dyes and metal ions from water

Vita Halysh [ID] · **Olena Sevastyanova** [ID] · **Stanislaw Pikus** [ID] · **Galina Dobele** [ID] · **Bogdan Pasalskiy** [ID] · **Volodymyr M. Gun'ko** [ID] · **Mykola Kartel** [ID]

Abstract Sugarcane bagasse (stalk) and straw (leaves), an agricultural waste, which had been subjected to either an organosolv or organosolv-oxidative pretreatment were used for the removal of methylene blue dye or heavy metals (Fe(III) and Cu(II)) from model aqueous solutions. The sorption of methylene blue was investigated as a function of pH, dye concentration, and contact time. The sorption of metal ions was studied as a function of concentration. Classical Langmuir and Freundlich adsorption models were used to analyze the sorption process. It was shown that adsorption isotherms fitted better into Freundlich isotherm model, which assumes a multilayer adsorption on a heterogeneous surface. The morphological, textural, and structural characteristics such as bulk and true densities, particle size distributions, porosity, and thermal decomposition features of the biosorbents were determined to understand better the mechanism of sorption of various pollutants. The results showed significant differences in the chemical compositions and physical properties of the initial and modified biomass samples, especially for the cellulosic biosorbents prepared with organosolv-oxidative pretreatment. For the removal of dyes, the

V. Halysh (✉)
Department of Ecology and Technology of Plant Polymers, Faculty of Chemical Engineering, Igor Sikorsky Kyiv Polytechnic Institute, Peremogy Avenu 37/4, Kyiv 03056, Ukraine
e-mail: v.galysh@gmail.com

V. Halysh · V. M. Gun'ko · M. Kartel
Chuiko Institute of Surface Chemistry, National Academy of Sciences of Ukraine, 17 General Naumov Street, Kyiv 03164, Ukraine

O. Sevastyanova (✉)
Department of Fiber and Polymer Technology, KTH Royal Institute of Technology, Teknikringen 56-58, 100 44 Stockholm, Sweden
e-mail: olena@kth.se

O. Sevastyanova
Department of Fiber and Polymer Technology, Wallenberg Wood Science Center, KTH Royal Institute of Technology, Teknikringen 56-58, 100 44 Stockholm, Sweden

S. Pikus
Faculty of Chemistry, Maria Curie-Sklodowska University, M. Curie-Sklodowska Sq. 3, 20-031 Lublin, Poland

G. Dobele
Latvian State Institute of Wood Chemistry, 27 Dzerbenes Str. LV, Riga 1006, Latvia

B. Pasalskiy
Kyiv National University of Trade and Economics, Kyoto str. 19, Kyiv 02156, Ukraine

development of a pore structure as a result of the pretreatment seemed to play an important role, while the sorption of metals was strongly dependent on the chemical composition of the biosorbent. The highest adsorption capacity for methylene blue and for Fe(III) and Cu(II) was obtained for a lignocellulosic sorbent from sugarcane straw prepared by organosolv pretreatment. The results obtained confirm a great potential use of agricultural waste from sugarcane industry in wastewater treatment.

Introduction

In the last decade, environmental protection has become a priority for scientists in many countries. Rapid industrial development contributes to environmental pollution with inorganic and organic toxic compounds that have a strong negative impact on the ecosystem (Tchounwou et al. 2012; Rajeswari and Sailaja 2014; Fazzo et al. 2017). The aim of the industrial treatment of wastewater is to reduce the discharge of various pollutants into the environment. Conventional techniques of water treatment to remove heavy metal ions include physicochemical and electrochemical methods such as reagent coagulation and precipitation (Hargreaves et al. 2018; Michel et al. 2019), ion exchange (Zhu et al. 2017; Hu and Boyer 2018), electrolysis (Kim et al. 2013), and membrane filtration (Khulbe and Matsuura 2018; Zheng et al. 2018). Common techniques that are used for the removal of dyes from wastewater, include biodegradation (Eslami et al. 2017), photocatalytic degradation (Salama et al. 2018), sonochemical degradation (Minero et al. 2008), membrane filtration (Salima et al. 2012), electrocoagulation (Mahmoud et al. 2013) and others. Despite the effectiveness of such methods, there are some disadvantages such as high reagent consumption, the generation of harmful sludge, complexity, high operational costs and high energy consumption.

Adsorption is considered to be one of the most appropriate methods to remove toxicants from aqueous media (Yagub et al. 2014; Renu and Singh 2017; Abtahi et al. 2018). The efficiency of adsorption

depends on the porosity of the sorbent and on the presence of surface functional groups as effective adsorption sites. The main problem with conventional sorbents with a developed porous structure, such as activated carbons, is the deterioration in their effectiveness due to the presence of solid particles in water that can enter the pores and reduce thus the adsorption capacity. These sorbents are also quite expensive.

In recent years, interest has increased towards biosorption based on the application of living (microorganisms) and non-living (plant materials) biomass (Gupta et al. 2015; Li et al. 2014; Kartel and Galysh 2017; Souza et al. 2018; Zhang et al. 2019). Microorganisms such as fungi, bacteria, and yeast cells have been proposed as biosorbents for water treatment (Gola et al. 2016; Mihaiescu et al. 2016; Xue et al. 2018). However, the treatment using living biomass is not widely used due to the fact that the cultivation of appropriate microorganisms is a costly process. Plant materials, such as wood, grasses and agricultural crops, are lignocellulosic complexes consisting of cellulose, hemicelluloses, lignin and other components in smaller quantities. The lignocellulosic materials show appropriate sorption properties due to their multicomponent composition and the presence of various active functionalities. The recycling of waste and by-products of the natural materials, especially agricultural wastes, into the biosorbents is considered to be a promising direction in chemical technology and ecology. The main advantages of biosorption are the availability of the raw materials, the simple operation, high efficiency, cheapness of the processes, and easy utilization of spent biosorbents by incineration (Galysh et al. 2017). The biosorption potential of various agro-industrial wastes, such as hazelnut hull (Sheibani et al. 2012), orange (Surovka and Pertile 2017) and grapefruit peel (Saeed et al. 2010), buckwheat hull (Li et al. 2012), sunflower seed shells (Suteu et al. 2010), walnut shells (Conrad et al. 2015), shells of almond (Pehlivan et al. 2009), and cotton waste (Ertaş et al. 2010) have been demonstrated by various researchers.

Chemical modification with organic and inorganic compounds can improve the sorption properties of biosorbents (Kumar et al. 2012). The treatment of plant raw materials with acetic acid and hydrogen peroxide at various ratios can affect their chemical composition greatly, resulting in lignocellulosic or cellulosic sorbents with different affinities toward

heavy metal ions and organic dyes (Halysh et al. 2018).

Sugarcane bagasse (stalk residue after juice extraction) is a low value by-product generated by the sugarcane industry that has been considered as a promising sorbent for wastewater treatment as it is or after certain chemical modification (Wong et al. 2009; Yu et al. 2013, 2015; Martin-Lara et al. 2010; Ho et al. 2005; Chandran et al. 2002). Sugarcane straw (leaves and stalk tips) is also generated in similar quantities to bagasse, corresponding to approximately 140 kg per one ton of sugarcane (Oliveira et al. 2013). However, despite a chemical composition similar to that of bagasse consisting also of cellulose, lignin, hemicelluloses and a somewhat higher amount of ash (Carvalho et al. 2015), significantly less attention has so far been paid to the sustainable use of this lignocellulosic material (Carvalho et al. 2016).

In this study, lignocellulosic and cellulosic biosorbents were prepared for the first time from both sugarcane bagasse and straw, organosolv pretreatment with glacial acetic acid or organosolv-oxidative pretreatment with a mixture of acetic acid and hydrogen peroxide being used for this purpose based on the optimal conditions assessed in our recent work (Halysh et al. 2019). Thorough characterization of the composition, physicochemical properties and pore structure was performed on the biosorbents before and after the pretreatments. The sorption of methylene blue from a model solution was investigated where parameters such as pH, contact time and concentration of dye were varied. The sorption of metal ions Fe(III) and Cu(II) was studied individually depending on their concentration in the aqueous solutions. The mechanism of adsorption of methylene blue was analyzed using the Langmuir or Freundlich models, the aim being to understand the relationships between the sorption and the physicochemical characteristics of biosorbents to find the most appropriate combinations of raw material and t pretreatment for certain types of pollutants.

Materials and methods

Materials

The sugarcane biomass, bagasse and straw (tips and leaves), was used as a precursor for biosorbent preparation. The initial chemical composition of the bagasse, straw, and related biosorbents was determined in accordance with TAPPI standards (T 222 cm-02 for lignin, T 211 om-02 for ash content, T 204 cm-97 for ethanol–benzene solubility). The cellulose content was determined according to the Kurschner–Hoffer method (Kurschner and Hoffer 1931). The holocellulose content was determined by chlorite method (Wise et al. 1946). Hemicelluloses content was calculated as the difference between the contents of holocellulose and cellulose. The total percentage of composition was calculated as the sum of extractives, lignin ash, holocellulose, and cellulose. Ground materials, 0.5 to 1 mm in particle size, were used for the chemical treatments.

Analytical grade hydrogen peroxide (H_2O_2 30%) and glacial acetic acid (CH_3COOH 99.7%) (Sigma-Aldrich, Germany) were used in the experiments. The Millipore-Milli Q system was used to purify water (up to ρ = 18 MΩ cm corresponding to ultrapure water).

Biosorbent preparation

Biosorbent preparation was carried out by subjecting biomass to the organosolv or oxidative-organosolv treatments following the methodology described in detail elsewhere (Halysh et al. 2018). Samples of sugarcane bagasse and straw were treated with glacial acetic acid and a mixture of acetic acid and hydrogen peroxide (70:30 vol/vol) at a solid to liquid ratio of 1:5, 90 °C for 2 h. The resulting materials after organosolv and oxidative-organosolv treatments were washed with deionized water, dehydrated, and dried at room temperature to a moisture content of 5–7 wt.%.

Biosorbent composition and structural characterization

The gravimetric method was used to determine the yield of the resulting biosorbents. The chemical composition of the sorbents was determined according to the TAPPI standards (as described above).

Fourier transform infrared (FTIR) spectroscopy with a Perkin-Elmer Spectrum 100 FTIR spectrometer equipped with a single reflection (attenuated total reflection, ATR) (Golden gate from Graseby Specac LTD, Kent, England) was used to evaluate structural changes in the sugarcane biomass after the treatments. Samples were analyzed at room temperature in the

4000–600 cm^{-1} range using 16 scans at a resolution of 4 cm^{-1} and intervals of 1 cm^{-1}.

The thermal stability of the biomass was measured using thermogravimetric analysis (TGA) with a Mettler Toledo TGA/DSC 1 instrument coupled with a STAR^e System. The temperature was raised from 25 to 600 °C (at a heating rate of 10 °C/min) in a nitrogen atmosphere. This temperature range is widely used for the TGA study of plant materials (Moriana et al. 2015; Oinonen et al. 2016).

A field-emission scanning electron microscope (FE-SEM) S-4800 (Hitachi, Japan) was used to study the surface morphology of the materials.

The textural characterization of the materials was carried out using the adsorption of benzene vapor in the desiccators (Keltsev 1991). To study the pore structure of the materials, the nitrogen adsorption/desorption isotherms (at 77.4 K) were recorded using a NOVA 2200 (Quantachrome, USA) instrument. The specific surface area was calculated according to the Brunauer–Emmett–Teller (BET) method with the assumption that the area occupied by a single nitrogen molecule is 0.162 nm^2. The pore volume and pore size distributions were determined using the Density Functional Theory (DFT) method (Volperts et al. 2019).

The bulk density of the materials was assessed using a glass cup with an internal volume (V_b) of 100 cm^3. The cup was filled with materials and weighed. The mass of a sample (m_s) was determined by subtracting the mass of the empty cup. The bulk density (ρ_b, g/cm^3) of materials was calculated as:

$$\rho_b = \frac{m_s}{V_b} \tag{1}$$

and the true density (ρ_t, g cm^{-3}) was determined as:

$$\rho_t = \frac{m_s}{V_t} \tag{2}$$

The small-angle X-ray scattering (SAXS) measurements were performed using a Panalytical Empyrean instrument (40 kV and 40 mA) with CuK$_\alpha$ radiation ($\lambda = 0.15418$ nm) and a SaxsWaxs configuration stage (transmission mode). The measurements were taken for the tested samples as well as for the empty cell. The scattering from the empty cell was then subtracted from the sample scattering curves (taking into account the absorption coefficients). In order to be able to compare the SAXS scattering curves, they were converted into identical experimental conditions (taking into account differences in absorption coefficients) (Brumberger 1965).

The differential pore size distribution (PSD) function $f(r)$ based on the SAXS data was calculated using Fredholm integral equation of the first kind for scattering intensity $I(q)$ (Pujari et al. 2007; Dieudonné et al. 2000; Fairén-Jiménez et al. 2006; Sakurai 2017) and was solved with a regularization procedure CONTIN (Provencher 1982) as described in Supplementary material (SM) file (Gun'ko 2014; Gun'ko et al. 2011, 2018; Goliszek et al. 2018). The particle size distribution functions (PaSD) were calculated using the SAXS data with a complex model with spherical, cylindrical and lamellar particles using a self-consistent regularization procedure giving the weight coefficient values for the contributions of the particles of different shapes (see SM file).

Effect of pH solution on sorption efficiency

The effect of pH on the efficiency of the methylene blue (MB) sorption onto initial and modified plant materials was investigated using 0.2 g of a sorbent and a dye solution with concentration of 100 mg/L. Solutions of 0.1 N hydrochloric acid and 0.1 N sodium hydroxide were used to adjust the solution pH. A spectrophotometric method was used to determine the initial and equilibrium concentrations. The transmission spectra were recorded using a Specord M-40 (Carl Zeiss) spectrophotometer at $\lambda = 664$ nm. A calibration graph was used for the determination initial and equilibrium concentrations of MB in solution. The concentrations of standard solutions were 10 mg/L, 20 mg/L, 30 mg/L, 40 mg/L, 50 mg/L, 60 mg/L, 70 mg/L, 80 mg/L, 90 mg/L, and 100 mg/L.

The efficiency of sorption (%) was calculated as:

$$Ef = \frac{(C_0 - C_e)}{C_o} 100 \tag{3}$$

where C_o and C_e are the initial and equilibrium concentrations of MB in solution, respectively (mg/L).

Kinetics studies

50 mL of MB solution was added to 0.2 g of a sorbent. The concentration of dye was 100 mg/L. The adsorption kinetics was studied using probes of 5 mL taken at

regular time intervals. After the measurement, the probes were returned back to the main solution. The kinetics study was performed for a period of 8 h.

The sorption capacity (mg/g) was calculated as:

$$q = \frac{(C_o - C_e)V}{m} \qquad (4)$$

where C_o and C_e are the initial and equilibrium concentrations, respectively, (mg/L); V is the volume of the solution (mL); and m is the mass of sorbent (g).

The pseudo-first-order (Moussout et al. 2018), pseudo-second-order (Azizian 2004), and interparticle diffusion (Weber and Morris 1963) models were used for the dye adsorption analysis. The linear forms of these models are:

$$ln(q_e - q_t) = lnq_e - \frac{k_1 t}{2.303} \qquad (5)$$

$$\frac{t}{q_t} = \frac{1}{k_2 q_e^2} + \frac{t}{q_e} \qquad (6)$$

$$q_t = k_3 t^{1/2} + C \qquad (7)$$

where q_e and q_t (mg/g) are the amounts of dye adsorbed at equilibrium and during time t (min), respectively; k_1 is the rate constant of pseudo-first-order adsorption (min^{-1}); k_2 is the rate constant of pseudo-second-order adsorption (mg/(g min)); k_3 is the rate constant of intraparticle diffusion adsorption (mg/(g min$^{1/2}$)); C is the boundary layer thickness (mg/g). The plots of $ln(q_e - q_t)$ versus t, t/q_t versus t and q_t versus $t^{1/2}$ were used to calculate the values of q_e and k_1, q_e and k_2, k_3 and n of the pseudo-first-order, the pseudo-first-order and intraparticle diffusion model, respectively. The best-fit model was selected according to the value of the coefficient of determination R^2.

Adsorption isotherms

0.4 g of sorbent was used to study the sorption capacity toward MB dye and 50 mL of model solution of a natural pH was added. The model solutions with different concentrations (30–900 mg/L) of MB were used. Diluted solutions of the dye were used for the determination of initial and equilibrium concentrations with the application of calibration graph. Experiments were carried out for 300 min.

The sorption of Fe(III) and Cu(II) species was studied using model solutions. The concentrations of Fe(III) and Cu(II) were 10–50 and 50–250 mg/L, respectively. The amount of sorbent was 0.5 g and the volume of the model solution was 50 mL; the time of sorption was 300 min. Iodometric determination of Cu(II) in solution (Brescia et al. 2012) and spectrophotometric method for Fe(II) determination (Li et al. 2013) were used to estimate the initial and equilibrium concentrations in solution.

The Langmuir and Freundlich isotherms were used to study the mechanisms of dye and metal species sorption:

$$\frac{C_e}{q_e} = \frac{1}{Q_m K_L} + \frac{C_e}{Q_m} \qquad (8)$$

$$logq_e = logK_F + \frac{lgC_e}{n} \qquad (9)$$

where C_e is the equilibrium concentration of adsorbate in solution (mg/L); q_e is the amount of adsorbate per mass unit of sorbent (mg/g); Q_m is the maximum adsorption capacity (mg/g); k_L is the Langmuir constant (L/mg); k_F is the Freundlich constant (L/g); and n is an empirical constant. The plots of C_e/q_e vs. C_e and $logq_e$ vs. $logC_e$ were used to calculate the values of Q_m and k_L, k_F and n, respectively. The feasibility of the adsorption was also evaluated by one of the essential characteristics of the Langmuir model R_L, which can be calculated as:

$$R_L = 1/(1 + K_L C_0) \qquad (10)$$

where C_0 is the highest initial dye concentration (mg/L).

All the experiments were performed in triplicates and the average values are used. Relative standard deviations were below 5%.

Results and discussion

Chemical composition of initial materials and biosorbents

Visual schemes of sugarcane biomass treatments with glacial acetic acid or a mixture of acetic acid and hydrogen peroxide and yields of biosorbents are shown in Fig. S3 (see SM file). The oxidative-organosolv treatment causes the removal of 47.9%

and 53.7% of the material by weight from initial bagasse and straw, respectively, and results in the formation of biosorbents of white color, which indicates a low lignin content in the product due to the biomass delignification with peracetic acid formed on interaction of acetic acid with hydrogen peroxide (Deykun et al. 2018). The removal of extractives of a different nature occurs also. The organosolv treatment results in a dark brown biosorbent due to the high residual lignin content. The loss of 11.2% and 21.4% of material by weight during the treatment of bagasse and straw, respectively, with acetic acid was due to the removal of extractives and ash. A partial removal of the polysaccharide components can also take place. A similar effect was observed during the treatment of apricot seed shells and walnut shells (Halysh et al. 2018).

The chemical composition of the materials depends strongly on the pretreatment conditions (Fig. 1).

Lignocellulosic sorbents are characterized by similar amounts of cellulose and lignin. Organosolv treatment with acetic acid leads to a decrease in the ash content and to slight increase in lignin content. The latter show less cellulose than the initial materials, which may indicate the depolymerization of high-molecular weight components into low-molecular weight ones since the amounts of hemicelluloses increased in both cases. The chemical composition of the biosorbents after the oxidative-organosolv treatment using a mixture of acetic acid and hydrogen peroxide confirmed the formation of cellulosic sorbents since the cellulose amount was higher than that in the initial materials and in the lignocellulosic biosorbents. The lignin content decreased significantly due to the oxidation and removal of the lignin. The oxidative-organosolv treatment resulted in a higher ash content for cellulosic sorbents compared to the initial materials.
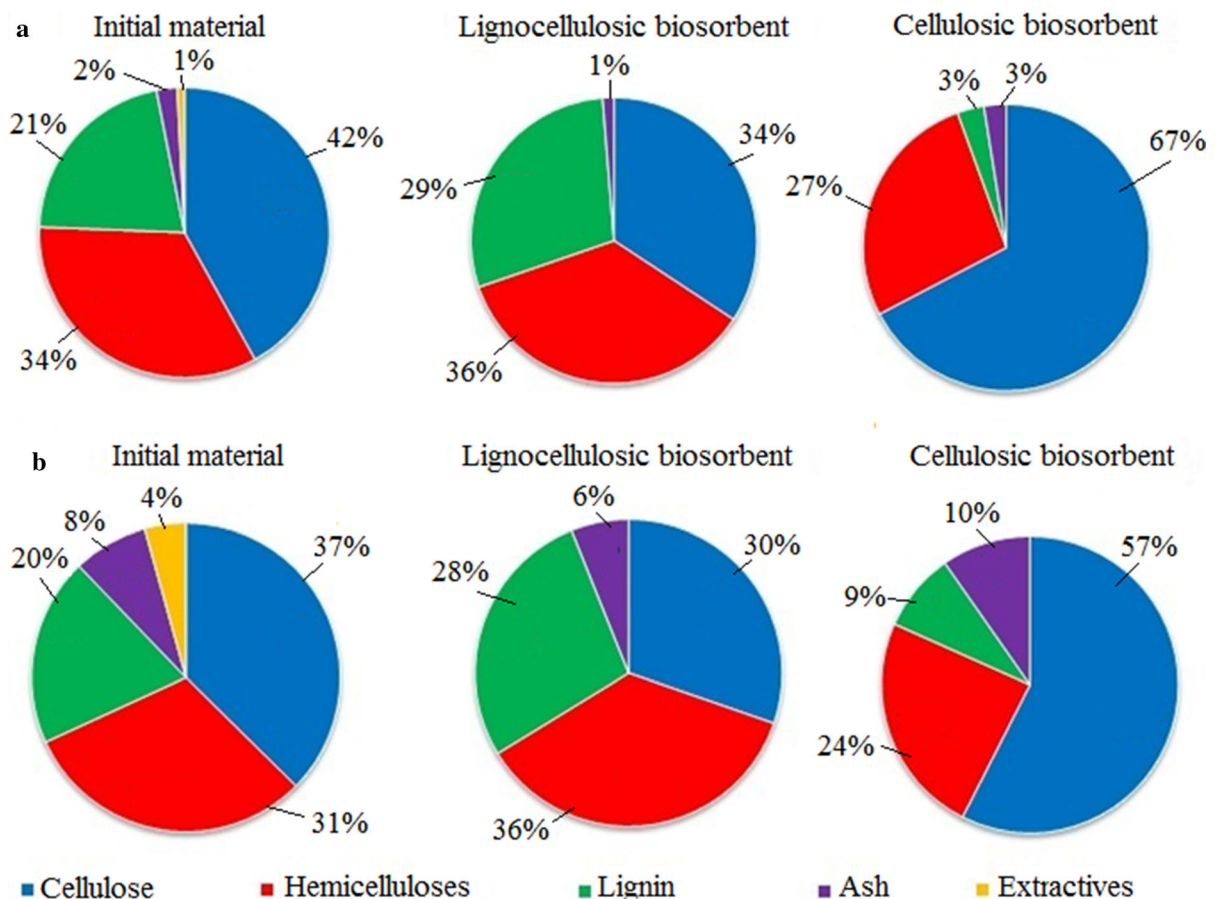
Fig. 1 Chemical composition of initial and modified materials: **a** bagasse-based materials, **b** straw-based materials

The FTIR spectra of the starting sugarcane biomass and of lignocellulosic sorbents are characterized by the presence of peaks for both aromatic and polysaccharide components as shown in Fig. S4 (see SM file). For example, lignin is characterized by a band at 1510–1513 cm^{-1} corresponding to the stretching vibrations of aromatic rings (Sun et al. 2004), as well as by a band within the aromatic out-of-plane region vibrations (900–700 cm^{-1}) (Drobniak and Mastalerz 2006). The peaks at 2924 and 2851 cm^{-1} can be attributed to the C-H stretching vibrations of the –CH_2– and –CH_3 groups of both lignin and esterified polysaccharide (Belmokaddem et al. 2011). The bands in the 1463–1430 cm^{-1} range can be assigned to the asymmetric aliphatic C–H deformation vibrations of the –CH_2– and –CH_3 groups (Drobniak and Mastalerz 2006). A peak at 1034 cm^{-1} can be assigned to the C–O and C–C stretching or C–OH bending vibrations in polysaccharides (Chaikumpollert et al. 2004). The stretching vibrations of the O–H groups of alcoholic and phenolic types (in the 3000–3700 cm^{-1} region), C–H stretching vibrations at 2924 cm^{-1} and water bending vibrations at 1641 cm^{-1} (Kačuráková et al. 1998) were also identified in the spectra (Fig. S4).

The main structural difference between the starting material and cellulosic sorbents was the absence of the bands assigned to lignin (1510–1513 cm^{-1} and 900–700 cm^{-1}) that confirms that the treatment leads to delignification of the materials.

Thermal analysis

The thermal stability of vegetable materials depends significantly on their chemical composition. Initial sugarcane biomass and biosorbents were studied using the TGA method (Fig. S5 in SM file). The TGA curves show that the materials underwent two different zones of thermal degradation. The first one (25–100 °C) corresponds to desorption of water (1.9–2.6 wt.%). The second one (200–450 °C) can be assigned to decomposition of the biomass resulting in 61.4–80.7 wt.% loss (dry basis). The biomass decomposition exhibited a behavior different from that of the initial biomasses and lignocellulosic sorbents. Although the changes are not obvious in the thermogravimetric curves (Fig. S5a, b), they become clear in the derivative curves (inserts in Fig. S5a, b). Two processes were observed in the second zone of the thermal degradation, especially for initial and lignocellulosic samples, due to the simultaneous and/or sequential decomposition of different chemical components caused by the associative desorption of water and the removal of CO and CO_2 formed from the material functionalities (since the TGA study was carried out in a nitrogen atmosphere with no oxygen).

The weight loss for sugarcane bagasse and straw on the first stage of the decomposition was 22.6% and 20.1%, respectively. For lignocellulosic sorbents, the values were higher, 28.2% and 25.9%, respectively. Cellulosic sorbents from straw showed a weight loss of only 10.8%, and for bagasse, only one decomposition process was found. The cellulosic sorbent from bagasse showed a significantly higher thermal stability than that of the other samples, but without any change in the temperature of the decomposition peak (Table S2). Initial sugarcane straw had the highest content of residues at 600 °C, irrespective of the sample type, probably because of a high inorganic content in this biomass (Carvalho et al. 2015).

Surface morphology characterization

SEM images (Fig. 2) show that the initial and treated materials have a complex particulate and surface morphologies. The surface of the raw bagasse and lignocellulosic material from bagasse contains micro-/macro-scaled pores. Treatment with acetic acid leads to a decrease in loose particles and the surface of lignocellulosic biosorbents becomes less heterogeneous (Fig. 2b, e) than that of the initial materials (Fig. 2a, d). After the treatment with hydrogen peroxide and acetic acid, the surface morphology of the cellulosic materials changed significantly (Fig. 2c, f) due to delignification.

Textural characterization

The nitrogen adsorption and benzene vapor sorption methods were used to investigate the texture of the materials. The nitrogen adsorption/desorption isotherms for the initial and treated materials (see Fig. S6 in SM file) had a shape corresponding to type IV of the IUPAC classification. The specific surface area, S_{BET} and total pore volume, V_p (Table 1) of the sugarcane biomass and biosorbents were small that indicates a strong compaction of biomacromolecules in these materials. After treatment, the S_{BET} value of the sugarcane bagasse-based materials decreased
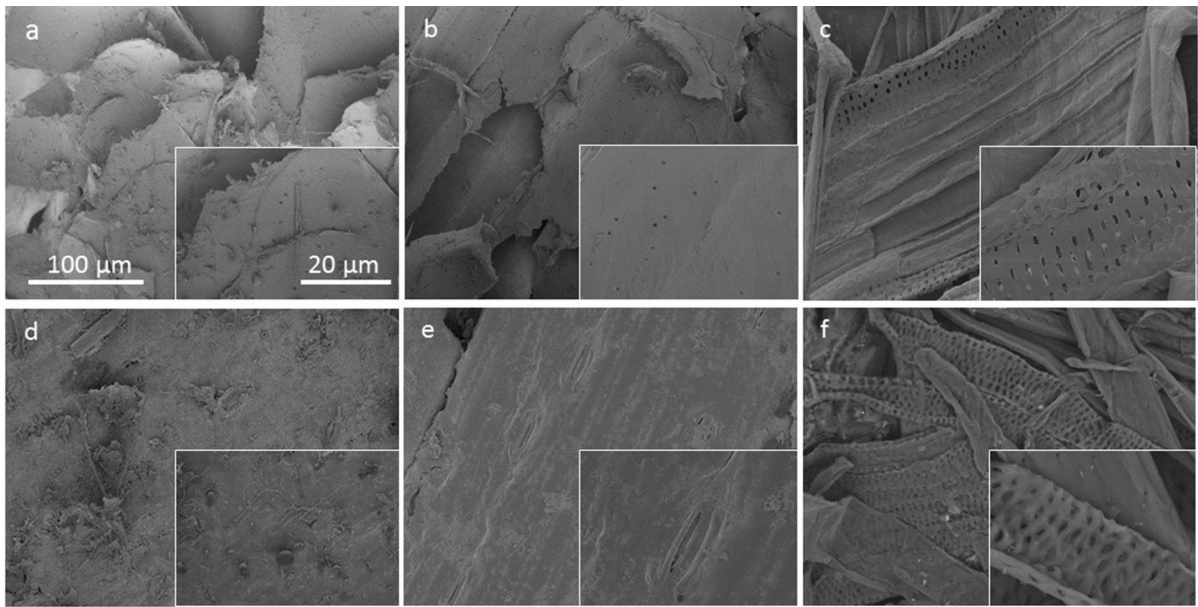
Fig. 2 SEM images for **a** initial bagasse and **d** straw and treated materials: lignocellulosic biosorbents from **b** bagasse and **e** straw and cellulosic biosorbents from **c** bagasse and **f** straw

Table 1 The surface characteristics and densities of the initial and treated sugarcane biomass

Parameters	Bagasse-based materials			Straw-based materials		
	IN	LC	C	IN	LC	C
S_{BET} (m^2/g)	1.4	1.2	1.3	1.9	2.7	5.4
Total pore volume $V_{p,n}$ (mm^3/g)	3.0	3.18	3.50	5.84	8.77	3.51
Micropore volume (mm^3/g)	0.43	0.42	0.38	0.64	0.97	0.37
Adsorption pore volume $V_{p,b}$ (mm^3/g)	80	110	150	50	180	130
Bulk density (g/cm^3)	0.049	0.116	0.048	0.087	0.124	0038
True density (g/cm^3)	0.096	0.383	0.069	0.138	0.487	0.119

IN initial material; *LC* lignocellulosic; *C* cellulosic

slightly and that of the sugarcane straw increased. The changes in the total pore volume were however rather the opposite. The treatment of straw leads to the formation of more porous materials than that for the bagasse biosorbents.

According to the benzene vapor sorption results (Table 1), the pore volumes ($V_{p,b}$) of the starting sugarcane bagasse and straw were 0.08 and 0.05 cm^3/g, respectively. After the oxidative-organosolv and oxidative treatments of the biomass, the $V_{p,b}$ value increased by factors of 1.4 and 2.8 for lignocellulosic and by factors of 1.7 and 2.2 for cellulosic sorbents from bagasse and straw, respectively. The $V_{p,b}$ values were much greater than the $V_{p,n}$ values (nitrogen adsorption), due to the ability of lignocellulosic

materials to swell in an organic (here benzene) solvent (Galysh et al. 2017).

The bulk and true densities of the initial and treated sugarcane bagasse and straw (Table 1) show significant differences. These values depend on the particle size distributions and their compaction. The bulk and true densities of the initial sugarcane straw were higher than that of the initial bagasse. However, for both samples, an increase in the values was observed after the acetic acid treatment, and a decrease is after the oxidative-organosolv treatment.

In contrast to the adsorption methods, the SAXS method gives the total textural characteristics related to both open and closed pores (in the range of 0.2–250 nm in pore radius). The textural characteristic values determined using the SAXS method could

therefore be much greater than those determined using the adsorption data, and this difference increases for strongly compacted materials (with restricted possibility of penetration of adsorbed molecules into the inner spaces of the compacted structures). The SAXS occurs at the surface of each biomacromolecule in any cavity between neighboring macromolecules or functionalities.

Both the pore size distributions (Fig. 3a, b) and particle size distributions (Fig. 3c, d) demonstrate that most of the pores are smaller than 10 nm in radius. This corresponds to the structures with cellulosic and lignocellulosic macromolecules.

These structures are characterized by the S_{SAXS} values between 561 and 617 m^2/g, which are much greater than the S_{BET} values because macromolecules are strongly compacted in microparticles (Fig. 2). The SAXS method senses the voids between the macromolecules in the microparticles. The similarity in the microstructures of the studied materials leads to a similarity in the chord (h) size distributions, CSD (corresponding to thickness of uniform fragments in the micro/macrostructures) at $h < 2$ nm (Fig. S2). However, the CSD were different at $h > 2$ nm and depend on the type of the treatment of the sorbents. On the whole, the initial and treated bagasse-based sorbents showed greater differences in the PSD (Fig. 3a) and CSD (Fig. S2) than the straw-based materials (Figs. 3b and S2). This difference is in agreement with the relatively stronger changes in the densities of the materials of the first series (Table 1).

Sorption of methylene blue

The sorption of methylene blue (MB) on the initial and modified materials was investigated as a function of pH, dye concentration and contact time (Fig. 4). The sorption efficiency of sugarcane residues as well as of lignocellulosic and cellulosic sorbents in removing MB as a function of pH value is shown in Fig. 4.

The pH value of the solution is one of the most important parameters that affects the adsorption process. The composition of the surface phase of biosorbents is not constant in the aqueous solution.
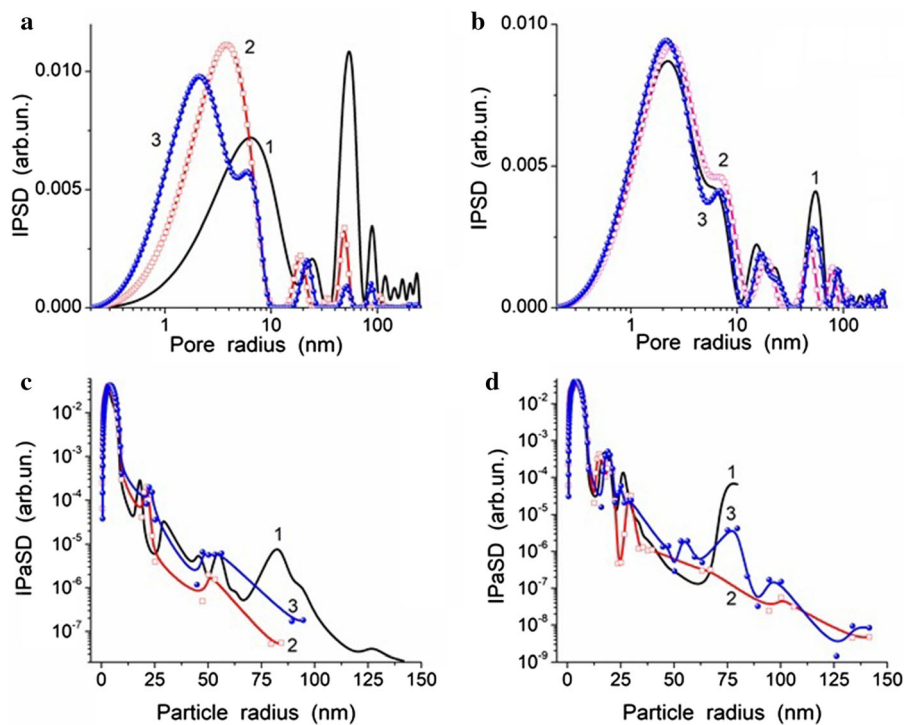
Fig. 3 a, **b** Incremental pore size distributions and **c**, **d** incremental particle size distributions calculated using the SAXS data for sugarcane bagasse (**a**, **c**, curves 1) and sugarcane straw (**b**, **d**, cuves 1), lignocellulosic biosorbents based on bagasse (**a**, **c**, curves 2) and straw (**b**, **d**, curves 2), and cellulosic biosorbents based on bagasse (**a**, **c**, curves 3) and straw (**b**, **d**, curves 3)
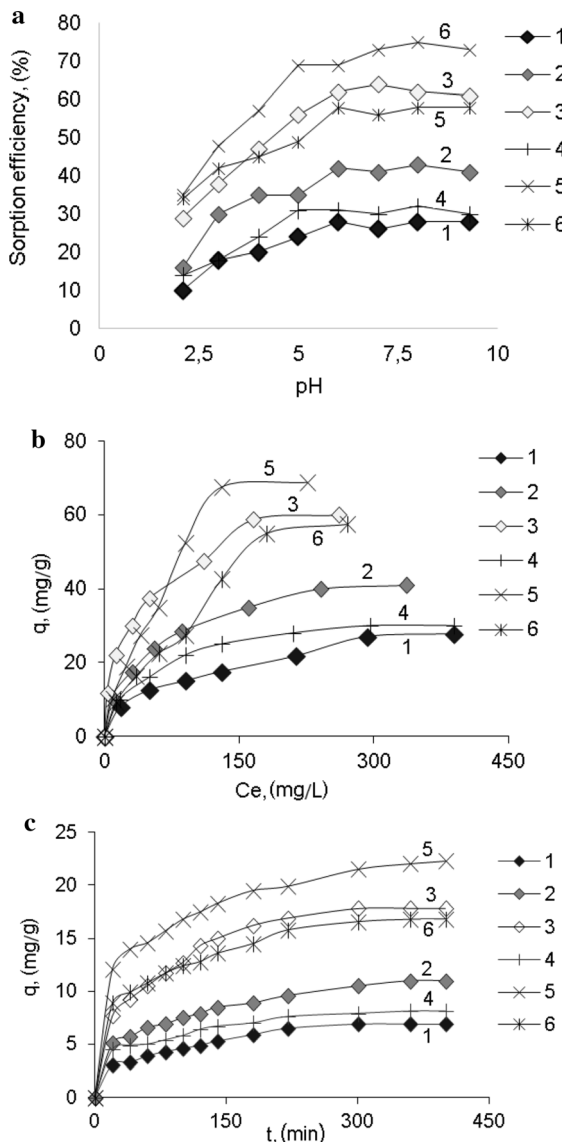
Fig. 4 Influence of **a** pH of solution, **b** initial concentration and **c** contact time on MB sorption onto: 1, 4 – initial bagasse and straw; 2, 5 – lignocellulosic biosorbents from bagasse and straw; 3, 6 – cellulosic biosorbents from bagasse and straw

Depending on pH, the surface of lignocellulose can exist in negative, neutral, or positive charge states due to the presence of different oxygen-containing functionalities such as aliphatic and phenolic hydroxyls, carbonyl and carboxyl groups. The MB dye is as positively charged cations upon dissolving in water (Boumediene et al. 2018). A decrease in the efficiency of the sorption of MB by lignocellulosic biosorbents at low pH is probably related to the presence of the

excess of H^+ ions (giving positively charged state of a surface) which are competing with the MB cations and repulsive forces take place (Fathy et al. 2013). Increase in pH leads to a deprotonation of carboxylic groups and, as a result, to change in the surface charge to negative one. The electrostatic repulsion forces between the positively charged MB and the biosorbent surface decreases, and new sorption sites are available for binding of MB. At the same time, not only electrostatic interactions but also van der Waals forces, hydrogen bonding and chemical bonding mechanisms can take place to capture MB (Liu et al. 2015). The maximum sorption is achieved at pH 7. The same results were obtained on brewers' spent grain (Kezerle et al. 2018) and modified jute (Manna et al. 2017).

The effect of MB concentration on the sorption onto initial and modified sugarcane bagasse and straw (Fig. 4) indicates that the chemical modification of sugarcane residues can improve the sorption properties of the resulted materials. For bagasse, the sorption capacity increased by a factor of 1.5 for the lignocellulosic sorbent and by a factor of 2.1 for the cellulosic sorbent. It is obvious that for bagasse-based biosorbents, the uptake of dye increases with increasing initial dye concentration from 50 to 400 mg/L. In the case of straw, the sorption capacity for the dye increases by a factor of 2.5 for the lignocellulosic sorbent and by a factor of 2.1 for the cellulosic sorbent. The uptake of dye increases with increasing dye concentration from 50 to 500 mg/L for the initial material, to 200 mg/L for cellulose-based and to 90 mg/L for lignocellulose-based sorbents. In general, the results show that the ability of the materials to sorb MB correlated with the adsorption pore volume. The dependence on adsorption pore volume of the sorption capacity of the sorbents to remove methylene blue from a model solution was: lignocellulose from straw (68.8 mg/g; 0.18 cm^3/g) > cellulose from bagasse (60 mg/g; 0.15 cm^3/g) > cellulose from straw (57.5 mg/g; 0.13 cm^3/g) > lignocellulose from bagasse (41 mg/g; 0.11 cm^3/g) > straw (30 mg/g; 0.08 cm^3/g) > bagasse (28 mg/g; 0.05 cm^3/g).

The results indicate that biosorbents are not inferior in sorption ability toward MB but even exceed that of other agro-industrial residues (sunflower seed shells (35.4 mg/g) (Suteu et al. 2010), oiltea shell (64.4 mg/g) (Liu et al. 2016), and corncob (18.3 mg/g) (Conrad et al. 2015)).

The classical adsorption Langmuir and Freundlich models were chosen to analyze the equilibrium between adsorbed and residue MB in the solution. The linear forms of the isotherms are widely used (Budnyak et al. 2018). The linear form of the Langmuir isotherm describes the monolayer adsorption onto a homogeneous surface at a constant temperature with no interactions between adsorbed molecules. The Freundlich isotherm describes a multilayer adsorption on a heterogeneous surface. The linear forms of the isotherms of the dye adsorption onto initial and modified sugarcane biomass are presented in Fig. S7 (SM file). The parameters for the Langmuir and Freundlich isotherms and the coefficients of determination R^2 are summarized in Table 2.

The values of R^2 suggest that the Langmuir model well fitted the adsorption processes with uniform adsorption and strong integrations between dye and adsorbent surface. The Q_m values were 33.6 mg/g and 33.2 mg/g for initial bagasse and straw, respectively, 36.5 mg/g and 102.0 mg/g for lignocellulosic sorbents from bagasse and straw, respectively, 114.9 mg/g and 93.4 mg/g for cellulosic sorbents from bagasse and straw, respectively. The values of K_L indicate a low affinity of MB for adsorption onto sugarcane residues. The R_L parameter can be used as a more reliable indicator of adsorption: if $0 < R_L < 1$ indicates favorable adsorption; $R_L > 1$ unfavorable adsorption; $R_L = 1$ linear adsorption; $R_L = 0$ indicates irreversible adsorption. For all the samples, the values of R_L (Table 2) were positive and small that indicates a highly favorable adsorption.

The adsorption results obtained are better described by the Freundlich isotherm model as high values of the coefficient of determination R^2 (0.9745–0.9944) were obtained for all the sorbents. For a favorable

adsorption process, the condition $0.1 < 1/n < 1$ must be met. For all samples, the value of $1/n$ was less than 1 and higher than 0.1 indicating a favorable adsorption of MB on sugarcane biomass. The K_F values (Table 2) indicate that lignocellulosic sorbent has the greatest ability to remove MB from the aqueous system.

To clarify the sorption mechanism, it is also important to study the process kinetics. Batch adsorption investigations were carried out with different contact times. Figure 4c shows the removal of MB from water by sugarcane biomass and other sorbents as a function of time. There is a rapid decrease in dye concentration during the first 20 min and thereafter the concentration gradually decreases more slowly during 300 min, presumably because the filling of pores of the sorbent leads to a retardation in the diffusion of the dye molecules deep into the pores. An equilibration time of 300 min is sufficient, since the maximum adsorption is reached during this period.

The applicability of the pseudo-first-order and pseudo-second-order models as well the intraparticle diffusion one was tested for methylene blue sorption onto the studied materials (Fig. S8). The parameters obtained from three kinetic models are given in Table 3.

The values of determination coefficient R^2 in the range of 0.9343–0.9818 confirm that the pseudo-first-order model does not provide a good fit for the adsorption of MB onto either the initial or modified sugarcane biomass, and the relationship between the dye concentration and the adsorption rate is nonlinear. The calculated equilibrium values did not match the experimental values. The plots (Fig. S8b) show that the relationship is linear. The calculated sorption capacities are close to the experimental values (Table 3). The coefficient determination R^2 is in range of 0.9902–0.9963 indicating that the pseudo-second-

Table 2 Parameters of isotherms of MB sorption onto initial and modified sugarcane residues	Type of isotherm	Parameters	Bagasese-based materials			Straw-based materials		
			IN	LC	C	IN	LC	C
	Langmuir	K_L (mg/L)	0.01	0.02	0.03	0.01	0.01	0.06
		Q_m (mg/g)	33.6	36.5	114.9	33.2	102.0	93.4
		R^2	0.9692	0.9731	0.9706	0.9736	0.9445	0.965
		R_L	0.1875	0.1081	0.083	0.1798	0.1928	0.2896
Note: IN – initial material; LC – lignocellulosic biosorbent; C – cellulosic biosorbent	Freundlich	K_F (L/g)	2.41	4.94	2.57	2.61	8.30	2.69
		$1/n$	0.41	0.38	0.37	0.39	0.64	0.64
		R^2	0.993	0.988	0.9899	0.9944	0.9745	0.98

Table 3 Parameters of kinetics of MB sorption onto initial and modified sugarcane residues

| Type of kinetics	Parameters	Bagasese-based materials			Straw-based materials		
		IN	LC	C	IN	LC	C
Pseudo-first-order	k_1 (min^{-1})	0.0106	0.071	0.012	0.0011	0.009	0.009
	q_e (mg/g)	5.8	6.6	14.89	11.6	13.0	10.75
	R^2	0.9299	0.9818	0.9818	0.9343	0.9758	0.9504
Pseudo-second-order	k_2 (mg/(g min)	0.0021	0.0015	0.0010	0.0026	0.0011	0.0013
	q_e (mg/g)	7.0	12.4	18.2	8.9	15.6	23.9
	R^2	0.9902	0.9909	0.9963	0.9943	0.9961	0.9948
Intraparticle diffusion	k_2 (mg/(g min$^{1/2}$)	0.27	0.40	0.68	0.25	0.66	1.2721
	C	1.86	3.44	5.66	3.31	9.87	1.6904
	R^2	0.9599	0.9889	0.9226	0.9608	0.9613	0.977

IN initial material; *LC* lignocellulosic biosorbent; *C* cellulosic biosorbent

order model is suitable for describing the kinetics of the adsorption of MB onto the studied materials.

According to the plot (Fig. S8c), the dependence of sorption capacities q_t on time $t^{0.5}$ is non-linear indicating that the chemical reaction controls the rate of adsorption of dye and its diffusion to a less degree. The coefficient R^2 (0.9226–0.9889) shows the deviation from linearity. The value of C is greater than zero indicating effect to some extend of boundary layer diffusion on the MB adsorption.

Metal cation sorption isotherms

Solutions with different concentrations of Fe(III) and Cu(II) species were used to investigate the effect of metal cation concentration on the sorption onto sugarcane biosorbents. The results (Fig. 5) show that both initial bagasse and straw have a lower sorption capacity toward metal ion species than the treated sorbents, due to the lack of accessible active adsorption sites. Treatment of the initial sugarcane residues with hydrogen peroxide in acetic acid at 90 °C leads to delignification, resulting in an increase in sorptivity due to the presence of oxygen-containing groups similar to those on a cellulosic surface. The highest sorption is observed for the lignocellulosic biosorbents due to the presence on their surface not only of functional groups of cellulose and hemicelluloses but also carboxylic- and phenolic-type groups of lignin (Guo et al. 2008; Shen et al. 2010).
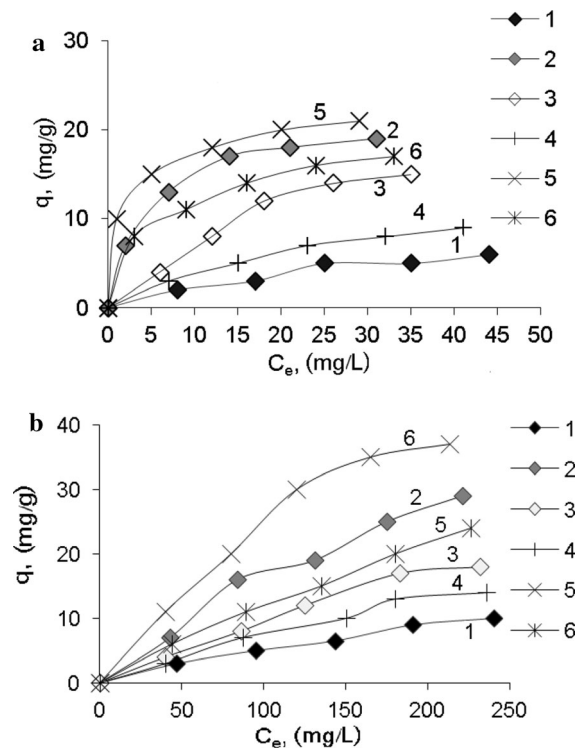
Fig. 5 Influence of initial Fe(III) (**a**) and Cu(II) (**b**) concentration on sorption capacity of the studied materials: 1, 4 – initial bagasse and straw; 2, 5 – lignocellulosic biosorbents from bagasse and straw; 3, 6 – cellulosic

The linear forms of the Langmuir and Freundlich isotherms for metal cation adsorption onto sugarcane residues and the prepared sorbents are shown in

Fig. S9 (SM file) and the relevant constants are given in Table 4.

The adsorption capacities calculated using the Langmuir model were 11.2, 21.7, and 21.7 mg/g for the initial bagasse and related lignocellulosic and cellulosic sorbents, respectively, and 15.6, 22.2, and 19.7 mg/g for the initial straw and related lignocellulosic and cellulosic sorbents, respectively. These values are close to the experimental adsorbed amounts during Fe(III) sorption, but the adsorption capacities for Cu(II) determined using the Langmuir model were 25.64, 93.46, and 81.30 mg/g for initial bagasse and related lignocellulosic and cellulosic sorbents, respectively, and 55.23, 85.47, and 89.28 mg/g for initial straw and related lignocellulosic and cellulosic sorbents, respectively. These values differ from the experimental values. As can be seen, the linear Langmuir isotherms, which were plotted as C_e/q_e vs. C_e values, with the determination coefficients (R^2) between 0.837–0.9919 and 0.6684–0.9056 for Fe(III) and Cu(II) sorption, respectively, are not adequate to describe the relationship between the adsorbed metal ions and their equilibrium concentration in the solution sorption occurred on a heterogeneous surface of lignocellulosic materials.

However, for the Freundlich isotherms, the values of R^2 were found to be 0.9904–0.9975 for the Fe(III) sorption and 0.9822–0.9989 for Cu(II) showing that the Freundlich isotherm model fitted well with the experimental data, as it shows higher R^2 values than the Langmuir model. Small values of $1/n$ imply stronger interaction between the adsorbent and heavy metal ions, while $1/n$ values between 0 and 1 indicate the identical adsorption process and adsorption energies for all sites. Smaller values of $1/n$ were obtained for the sorption of metals ions onto the lignocellulosic sorbents.

The sorption capacities toward Fe(III) and Cu(II) are competitive with other lignocellulosic residues, for example, the sorption capacity of orange peel and hazelnut hull towards Fe(III) is 13.3 mg/g and 13.6 mg/g, respectively (Sheibani et al. 2012; Surovka and Pertile 2017), and the sorption capacity of orange peel, grape seed, peanut shell towards Cu(II) is 4.6 mg/g, 3.4 mg/g and 25.4 mg/g, respectively (Surovka and Pertile 2017; Bsoul et al. 2014; Mathew et al. 2016).

Conclusion

Two types of biosorbents (lignocellulosic and cellulosic) were prepared based on chemical pre-treatment (organosolv or organosolv-oxidative) of the major sugarcane by-products, bagasse and straw. Comparison of the starting and chemically treated sorbents demonstrated that the sorption properties of the materials toward methylene blue depended on the

Table 4 Parameters of isotherms of Fe(III) and Cu(II) sorption onto initial and modified materials

Type of kinetics	Parameters	Bagasese-based materials			Straw-based materials		
		IN	LC	C	IN	LC	C
Fe(III) sorption							
Langmuir	K_L (mg/L)	0.025	0.23	0.025	0.03	0.49	0.17
	Q_m (mg/g)	11.2	21.7	21.7	15.6	22.2	19.7
	R^2	0.9211	0.9893	0.837	0.9801	0.988	0.9919
Freundlich	K_F (L/g)	1.55	2.71	1.29	1.58	4.47	3.07
	$1/n$	0.52	0.18	0.96	0.89	0.098	0.18
	R^2	0.992	0.9975	0.9905	0.9904	0.9945	0.9935
Cu(II) sorption							
Langmuir	K_L (mg/L)	0.002	0.002	0.001	0.002	0.004	0.002
	Q_m (mg/g)	25.64	93.46	81.30	55.23	85.47	89.28
	R^2	0.8755	0.6848	0.6953	0.6684	0.8911	0.9056
Freundlich	K_F (L/g)	1.33	1.18	1.22	1.13	1.18	1.32
	$1/n$	0.16	0.12	0.13	0.72	0.144	0.41
	R^2	0.9932	0.9853	0.9853	0.9822	0.9989	0.9911

IN initial material; *LC* lignocellulosic biosorbent; *C* cellulosic biosorbent

adsorption pore volume that could be related to the accessibility of active adsorption sites. The highest sorption capacity towards methylene blue was achieved for the lignocellulosic sorbent from straw, which had the highest value of adsorption pore volume. The lignocellulosic sorbent from bagasse, which had the lowest value of adsorption pore volume had the lowest sorption capacity towards methylene blue dye. The dependence of the sorption capacity for methylene blue and the adsorption pore volume of various sorbents was in the following order: lignocellulosic sorbent from straw (68.8 mg/g; 0.18 cm^3/g) > cellulosic sorbent from bagasse (60 mg/g; 0.15 cm^3/g) > cellulosic sorbent from straw (57.5 mg/g; 0.13 cm^3/g) > lignocellulosic sorbent from bagasse (41 mg/g; 0.11 cm^3/g) > initial straw (30 mg/g; 0.08 cm^3/g) > initial bagasse (28 mg/g; 0.05 cm^3/g). However, the sorption properties toward metal species depended more strongly on the chemical composition of the sorbents. Lignocellulosic sorbents from bagasse and straw had the highest sorption capacity for Fe(III) and Cu(II) (19 and 21 mg/g, 29 and 37 mg/g, respectively) due to the presence on their surface not only of functional groups of cellulose and hemicelluloses but also carboxylic- and phenolic-type groups of lignin. The adsorption isotherms fit better with the Freundlich isotherm and pseudo-second-order models, suggesting a multilayer adsorption on a heterogeneous surface. The optimal pH values for the methylene blue sorption was found to be at 6 and higher. In general, the greatest sorption capacity for Fe(III) and Cu(II) (21 and 37 mg/g, respectively) and methylene blue (68.8 mg/g) were obtained for the lignocellulosic sorbent from sugarcane straw.

Compliance with ethical standards

Conflict of interest The authors declare that they have no conflict of interest.

References

Abtahi M, Fakhri Y, Sarafraz M, Keramati H, Conti GO, Ferrante M, Amanidaz N, Pouya RH, Moradi B, Baninameh Z (2018) Removal of cesium through adsorption from aqueous solutions: a systematic review. J Adv Environ Health Res 6:96–106. https://doi.org/10.22102/jaehr.2018.104959.1048

Azizian S (2004) Kinetic models of sorption: a theoretical analysis. J Colloid Interface Sci 276:47–52. https://doi.org/10.1016/j.jcis.2004.03.04

Belmokaddem F-Z, Pinel C, Huber P, Petit-Conil M, Da Silva Perez D (2011) Green synthesis of xylan hemicellulose esters. Carbohydr Res 346(18):2896–2904. https://doi.org/10.1016/j.carres.2011.10.012

Boumediene M, Benaïssa H, George B, Molina S, Merlin A (2018) Effects of pH and ionic strength on methylene blue removal from synthetic aqueous solutions by sorption onto orange peel and desorption study. J Mater Environ Sci 9:1700–1711. https://doi.org/10.26872/jmes.2018.9.6.190

Brescia F, Arents J, Meslich H, Turk A (2012) Fundamentals of chemistry: laboratory studies, University of Denver, Academic Press

Brumberger H (1965) Small angle x-ray scattering. Gordon and Breach, New York, Syracuse

Bsoul AA, Zeatoun L, Abdelhay A, Chiha M (2014) Adsorption of copper ions from water by different types of natural seed materials. Desalin Water Treat 52:5876–5882. https://doi.org/10.1080/19443994.2013.808593

Budnyak TM, Aminzadeh S, Pylypchuk IV, Sternik D, Tertykh VA, Lindström ME, Sevastyanova O (2018) Methylene Blue dye sorption by hybrid materials from technical lignins. J Environ Chem Eng 6:4997–5007. https://doi.org/10.1016/j.jece.2018.07.041

Carvalho DM, Sevastyanova O, Penna LS, Silva BP, Lindström ME, Colodett JL (2015) Assessment of chemical transformation in eucalyptus, sugarcane bagasse and straw during hydrothermal, dilute acid, and alkaline pretreatments. Ind Crop Prod 73:118–126. https://doi.org/10.1016/j.indcrop.2015.04.021

Carvalho DMD, Sevastyanova O, Queiroz JHD, Colodette JL (2016) Cold alkaline extraction as a pretreatment for bioethanol production from eucalyptus, sugarcane bagasse and sugarcane straw. Energy Convers Manag 124:315–324. https://doi.org/10.1016/j.enconman.2016.07.029

Chaikumpollert O, Methacanon P, Suchiva K (2004) Structural elucidation of hemicelluloses from Vetiver grass. Carbohydr Polym 57:191–196. https://doi.org/10.1016/j.carbpol.2004.04.011

Chandran CB, Singh D, Nigam P (2002) Remediation of textile effluent using agricultural residues. Appl Biochem Biotech 102–103:207–212. https://doi.org/10.1385/ABAB:102-103:1-6:207

Conrad EK, Nnaemeka OJ, Chris AO (2015) Adsorption removal of Methylene Blue from aqueous solution using agricultural waste: equilibrium, kinetic and thermodynamic studies. Am J Chem Mater Sci 2:14–15

Deykun I, Halysh V, Barbash V (2018) Rapeseed straw as an alternative for pulping and papermaking. Cellulose Chem Technol 52:833–839

Drobniak A, Mastalerz M (2006) Chemical evolution of Miocene wood: example from the Belchatow brown coal deposit, central Poland. Int J Coal Geol 66:157–178

Dieudonné Ph, Hafidi AA, Delord P, Phalippou J (2000) Transformation of nanostructure of silica gels during drying. J Non-Crystal Solid 262:155–161. https://doi.org/10.1016/S0022-3093(99)00687-0

Ertaş M, Acemioğlu B, Alma MH, Usta M (2010) Removal of methylene blue from aqueous solution using cotton stalk, cotton waste and cotton dust. J Hazard Mater 183:421–427. https://doi.org/10.1016/j.jhazmat.2010.07.041

Eslami H, Khavidak SS, Salehi F, Khosravi R, Ali Fallahzadeh R, Peirovi R, Sadeghi S (2017) Biodegradation of methylene blue from aqueous solution by bacteria isolated from contaminated soil. J Adv Environ Health Res 5:10–15

Fairén-Jiménez D, Carrasco-Marín F, Djurado D, Bley F, Ehrburger-Dolle F, Moreno-Castilla C (2006) Surface area and microporosity of carbon aerogels from gas adsorption and small- and wide-angle X-ray scattering measurements. J Phys Chem B 110:8681–8688. https://doi.org/10.1021/jp055992f

Fathy NA, El-Shafey OI, Khalil LB (2013) Effectiveness of alkali-acid treatment in enhancement the adsorption capacity for rice straw: the removal of methylene blue dye. Phys Chem. https://doi.org/10.1155/2013/208087

Fazzo L, Minichilli F, Santoro M, Ceccarini A, Seta MD, Bianchi F, Comba P, Martuzzi M (2017) Hazardous waste and health impact: a systematic review of the scientific literature. Environ Health 16:107. https://doi.org/10.1186/s12940-017-0311-8

Galysh V, Sevastyanova O, Kartel M, Lindström M, Gornikov Yu (2017) Impact of ferrocyanide salts on the thermo-oxidative degradation of lignocellulosic sorbents. J Therm Anal Calorim 128:1019–1025. https://doi.org/10.1007/s10973-016-5984-7

Gola D, Dey P, Bhattacharya A, Mishra A, Malik A, Namburath M, Ahmmad SZ (2016) Multiple heavy metal removal using an entomopathogenic fungi Beauveria bassiana. Bioresour Technol. https://doi.org/10.1016/j.biortech.2016.06.096

Goliszek M, Podkościelna B, Fila K, Riazanova AV, Aminzadeh S, Sevastyanova O, Gun'ko VM (2018) Synthesis and structure characterization of polymeric nanoporous microspheres with lignin. Cellulose 25:5843–5862. https://doi.org/10.1007/s10570-018-2009-7

Gun'ko VM (2014) Composite materials: textural characteristics. Appl Surf Sci 307:444–454. https://doi.org/10.1016/j.apsusc.2014.04.055

Gun'ko VM, Meikle ST, Kozynchenko OP, Tennison SR, Ehrburger-Dolle F, Morfin I, Mikhalovsky SV (2011) Comparative characterization of carbon and polymer adsorbents by SAXS and nitrogen adsorption methods. J Phys Chem C 115:10727–10735. https://doi.org/10.1021/jp201835r

Gun'ko VM, Turov VV, Pakhlov EM, Krupska TV, Charmas B (2018) Effect of water content on the characteristics of hydro-compacted nanosilica. Appl Surf Sci 459:171–178. https://doi.org/10.1016/j.apsusc.2018.07.213

Guo X, Zhang S, Shan X (2008) Adsorption of metal ions on lignin. J Hazard Mater 151:134–142. https://doi.org/10.1016/j.jhazmat.2007.05.065

Gupta VK, Nayak A, Agarwal S (2015) Bioadsorbents for remediation of heavy metals: current status and their future prospects. Environ Eng Res 20:1–18. https://doi.org/10.4491/eer.2015.018

Halysh V, Trembus I, Deykun I, Ostapenko A, Nikolaichuk A, Ilnitska G (2018) Development of effective technique for the disposal of the Prunus Armeniaca seed shells. Eastern-EurJ Enterprise Technol 1:4–9

Halysh V, Sevastyanova O, de Carvalho DM, Riazanova AV, Lindström ME, Gomelya M (2019) Effect of oxidative treatment on composition and properties of sorbents prepared from sugarcane residues. Ind Crop Prod 139:111566. https://doi.org/10.1016/j.indcrop.2019.111566

Hargreaves AJ, Vale P, Whelan J, Alibardi L, Constantino C, Dotro G, Cartmell E, Campo P (2018) Coagulation–flocculation process with metal salts, synthetic polymers and biopolymers for the removal of trace metals (Cu, Pb, Ni, Zn) from municipal wastewater. Clean Technol Envir 20:393–402. https://doi.org/10.1007/s10098-017-1481-3

Ho Y-S, Chiu W-T, Wang C-C (2005) Regression analysis for the sorption isotherms of basic dyes on sugarcane dust. Bioresour Technol 96:1285–1291

Hu Y, Boyer TH (2018) Removal of multiple drinking water contaminants by combined ion exchange resin in a completely mixed flow reactor. J Water Supply Res Technol Aqua 67:659–672. https://doi.org/10.2166/aqua.2018.101

Kartel M, Galysh V (2017) New composite sorbents for caesium and strontium ions sorption. Chem J Moldova 12:45–54

Kačuráková M, Belton PS, Wilson RH, Hirsch J, Ebringerová A (1998) Hydration properties of xylan-type structures: an FTIR study of xylooligosaccharides. J Sci Food Agric 77:38–44. https://doi.org/10.1002/(sici)1097-0010(199805)77:1<38::aid-jsfa999>3.0.co;2-5

Keltsev NV (1991) Fundamentals of adsorption technology. Chimia, Moscow (in Russian)

Kezerle A, Velić N, Hasenay D, Kovačević D (2018) Lignocellulosic materials as dye adsorbents: adsorption of methylene blue and congo red on Brewers' spent grain. Croat Chem Acta 91:53–64. https://doi.org/10.5562/cca3289

Khulbe KC, Matsuura T (2018) Removal of heavy metals and pollutants by membrane adsorption techniques. Appl Water Sci 8:19. https://doi.org/10.1007/s13201-018-0661-6

Kim DG, Kim WY, Yun CY, Son DJ, Chang D, Bae HS, Lee YH, Young Y, Sunwoo Y, Hong KH (2013) Agro-industrial wastewater treatment by electrolysis technology. Int J Electrochem Sci 8:9835–9850

Kumar PS, Ramalingam S, Abhinaya RV, Kirupha SD, Murugesan A, Sivanesan S (2012) Adsorption of metal ions onto the chemically modified agricultural waste. Clean: Soil, Air, Water 40:188–197. https://doi.org/10.1002/clen.201100118

Kurschner K, Hoffer A (1931) A new quantitative cellulose determination. Chem Zeit 55:1811

Li N, Hefferren JJ, Li K (2013) Quantitative chemical analysis. World Scientific Pub Co Inc, Singapore

Li K, Wang Q, Dang Y, Wei H, Luo Q, Zhao F (2012) Characteristic and mechanism of Cr(VI) biosorption by buckwheat hull from aqueous solutions. Acta Chim Sinica 70:929–935. https://doi.org/10.6023/A1108242

Li J, Li Y, Wu Y, Zheng M (2014) A comparison of biochars from lignin, cellulose and wood as the sorbent to an aromatic pollutant. J Hazard Mater 280:450–457. https://doi.org/10.1016/j.jhazmat.2014.08.033

Liu L, Gao ZL, Su XP, Chen X, Jiang L, Yao JM (2015) Adsorption removal of dyes from single and binary solutions using a cellulose-based bioadsorbent. ACS Sustain Chem Eng 3:432–442

Liu J, Li E, You X, Hu C, Huang Q (2016) Adsorption of methylene blue on an agro-waste oiltea shell with and without fungal treatment. Sci Rep 6:1–10. https://doi.org/10.1038/srep38450

Mahmoud MS, Farah JY, Farrag TE (2013) Enhanced removal of Methylene Blue by electrocoagulation using iron electrodes. Egyptian J Pet 22:211–216. https://doi.org/10.1016/j.ejpe.2012.09.013

Manna S, Roy D, Saha P, Gopakumar D, Thomas S (2017) Rapid methylene blue adsorption using modified lignocellulosic materials. Process Saf Environ Prot 107:346–356. https://doi.org/10.1016/j.psep.2017.03.008

Martin-Lara MA, Rico IR, Vicente ICA, Garcia GB, Hoces MC (2010) Modification of the sorptive characteristics of sugarcane bagasse for removing lead from aqueous solution. Desalination 256:58–63

Mathew BB, Jaishankar M, Biju VG, Beeregowda KN (2016) Role of bioadsorbents in reducing toxic metals. J Toxicol 12:1–13. https://doi.org/10.1155/2016/4369604

Michel MM, Tytkowska M, Reczek L, Trach Y, Siwiec T (2019) Technological conditions for the coagulation of wastewater from cosmetic industry. J Ecol Eng 20:78–85. https://doi.org/10.12911/22998993/105333

Mihaiescu T, Stanila A, Odagiu A, Mihaiescu R (2016) Assessment of copper and lead biosorption from aqueous solutions by Brewer's yeast. ProEnvironment 9:430–434

Minero C, Pellizzari P, Maurino V, Pelizzetti E, Vione D (2008) Enhancement of dye sonochemical degradation by some inorganic anions present in natural waters. Appl Catal B 77:308–316. https://doi.org/10.1016/j.apcatb.2007.08.001

Moriana R, Vilaplana F, Ek M (2015) Forest residues as renewable resources for bio-based polymeric materials and bioenergy: chemical composition, structure and thermal properties. Cellulose 22:3409–3423. https://doi.org/10.1007/s10570-015-0738-4

Moussout H, Ahlafi H, Aazza M, Maghat H (2018) Critical of linear and nonlinear equations of pseudo-first order and pseudo-second order kinetic models. Karbala Int J Mod Sci 4:244–254. https://doi.org/10.1016/j.kijoms.2018.04.001

Oinonen P, Krawczyk H, Ek M, Henriksson G, Moriana R (2016) Bioinspired composites from cross-linked galactoglucomannan and microfibrillated cellulose: Thermal, mechanical and oxygen barrier properties. Carbohydr Polym 136:146–153. https://doi.org/10.1016/j.carbpol.2015.09.038

Oliveira FMV, Pinheiro IO, Souto-Maior AM, Martin C, Golcalves AR, Rocha GJM (2013) Industrial-scale steam explosion pretreatment of sugarcane straw for enzymatic hydrolysis of cellulose for production of second generation ethanol and value-added products. Bioresour Technol 130:168–173

Pehlivan E, Altun T, Cetin S, Bhanger MI (2009) Lead sorption by waste biomass of hazelnut and almond shell. J Hazard Mater 167:1203–1208. https://doi.org/10.1016/j.jhazmat.2009.01.126

Provencher SW (1982) A constrained regularization method for inverting data represented by linear algebraic or integral equations. Comp Phys Comm 27:213–227. https://doi.org/10.1016/0010-4655(82)90173-4

Pujari PK, Sen D, Amarendra G, Abhaya S, Pandey AK, Dutta D (2007) Study of pore structure in grafted polymer membranes using slow positron beam and small-angle X-ray scattering techniques. Nuclear Instrum Method Phys Res B 254:278–282. https://doi.org/10.1016/j.nimb.2006.11.052

Rajeswari TR, Sailaja N (2014) Impact of heavy metals on environmental pollution. J Chem Pharm Sci 3:117–181

Renu AM, Singh K (2017) Heavy metal removal from wastewater using various adsorbents: a review. J Water Reuse Desal 7:387–419. https://doi.org/10.2166/wrd.2016.104

Saeed A, Sharif M, Iqbal M (2010) Application potential of grapefruit peel as dye sorbent: kinetics, equilibrium and mechanism of crystal violet adsorption. J Hazard Mater 179:564–572. https://doi.org/10.1016/j.jhazmat.2010.03.041

Sakurai S (2017) SAXS evaluation of size distribution for nanoparticles, in X-ray Scattering; Ares, A.E. Ed.; InTech: Croatia. https://doi.org/10.5772/105981

Salama A, Mohamed A, Aboamera NM, Osman TA, Khattab A (2018) Photocatalytic degradation of organic dyes using composite nanofibers under UV irradiation. Appl Nanosci 8:155–161. https://doi.org/10.1007/s13204-018-0660-9

Salima A, Ounissa K-S, Lynda M, Mohamed B (2012) Cationic dye (MB) removal using polymer inclusion membrane (PIMs). Proc Eng. 33:38–46. https://doi.org/10.1016/j.proeng.2012.01.1174

Sheibani A, Shishehbor MR, Alaei H (2012) Removal of Fe(III) ions from aqueous solution by hazelnut hull as an adsorbent. Int J Ind Chem 3:4. https://doi.org/10.1186/2228-5547-3-4

Shen Y-S, Wang S-L, Huang S-T, Tzou Y-M, Huang J-H (2010) Biosorption of Cr(VI) by coconut coir: spectroscopic investigation on the reaction mechanism of Cr(VI) with lgnocellulosic material. J Hazard Mater 179:160–165. https://doi.org/10.1016/j.jhazmat.2010.02.073

Souza WDM, Rodriques WS, Lima Filho MMS, Alves JJF, Oliveira MBF (2018) Heavy metals uptake on Malpighia emarginata D.C. seed fiber microparticles: physicochemical characterization, modeling and application in landfill leachate. Waste Manag 78:356–365. https://doi.org/10.1016/j.wasman.2018.06.004

Sun JX, Sun XF, Sun RC, Su YQ (2004) Fractional extraction and structural characterization of sugarcane bagasse hemicelluloses. Carbohydr Polym 56:195–204. https://doi.org/10.1016/j.carbpol.2004.02.002

Surovka D, Pertile E (2017) Sorption of iron, manganese, and copper from aqueous solution using orange peel: optimization, isothermic, kinetic, and thermodynamic studies. Polish J Environ Stud 26:795–800. https://doi.org/10.15244/pjoes/60499

Suteu D, Zaharia C, Badeanu M (2010) Agriculture wastes used as sorbents for dyes removal from aqueous environments. Lucrari Stiintifice 53:140–145

Tchounwou PB, Yedjou CG, Patloll AK, Sutton DJ (2012) Heavy metals toxicity and the environment. Exp Suppl 101:133–164. https://doi.org/10.1007/978-3-7643-8340-4_6

Volperts A, Plavniece A, Dobele G, Zhurinsh A, Kruusenberg I, Kaare K, Locs J, Tamasauskaite-Tamasiunaite L, Norkus E (2019) Biomass based activated carbons for fuel cells. Renew Energy 141:40–45. https://doi.org/10.1016/j.renene.2019.04.002

Weber WJ, Morris JC (1963) Kinetics of adsorption on carbon from aqueous solutions. J Sanit Eng Div 89:31–60

Wise LE, Merphy M, D'Addieco AA (1946) Chlorite holocellulose, its fraction and bearing on summative wood analysis and on studies on the hemicelluloses. Paper Trad J 122:35–43

Wong SY, Tan YP, Abdullah AH, Ong ST (2009) The removal of basic and reactive dyes using quartenised sugar cane bagasse. J Phys Sci 20:59–74

Xue C, Qi P, Liu Y (2018) Adsorption of aquatic Cd^{2+} using a combination of bacteria and modified carbon fiber. Adsorpt Sci Technol 36:857–871. https://doi.org/10.1177/0263617417724946

Yagub MT, Sen TK, Afroze S, Ang HM (2014) Dye and its removal from aqueous solution by adsorption: a review. Adv Colloid Interface 209:172–184

Yu L-X, Wang L-Y, Chi R-A, Zhang Y-F, Xu Z-G, Guo J (2013) Competitive adsorption of Pb^{2+} and Cd^{2+} on magnetic modified sugarcane bagasse prepared by two simple steps. Appl Surf Sci 268:163–170

Yu L-X, Zhu J, Feng L-Y, Chu R-A (2015) Simultaneous removal of cationic and anionic dyes by the mixed sorbents of magnetic and non-magnetic modified sugarcane bagasse. J Colloid Interface Sci 451:153–160

Zhang L, Li W, Cao H, Hu D, Chen X, Guan Y, Tang J, Gao H (2019) Ultra-efficient sorption of Cu^{2+} and Pb^{2+} ions by light biochar derived from Medulla tetrapanacis. Bioresour Technol 291:121818. https://doi.org/10.1016/j.biortech.2019.121818

Zheng J, Yan K, Wu Z, Liu M, Wang Z (2018) Removal of sulfanilic acid from water using a low-pressure electrochemical RuO_2-TiO_2@Ti/PVDF composite membrane. Front Chem 6:395. https://doi.org/10.3389/fchem.2018.00395

Zhu C, Wang Q, Pang W, Wang Z, Cao J, Hu W (2017) Mechanisms of phosphorus removal from wastewater by ion exchange resin. Desalin Water Treat 79:347–355. https://doi.org/10.5004/dwt.2017.20890